Review of Geant4-DNA applications for micro and nanoscale simulations

S. Incerti, M. Douglass, S. Penfold, S. Guatelli, E. Bezak

Review of Geant4-DNA applications for micro and nanoscale simulations

S Incerti[1,2], M Douglass[3, 4], S Penfold[3, 4], S Guatelli[5,6], E Bezak[4,7,8]

[1]Univ. Bordeaux, CENBG, UMR 5797, F-33170 Gradignan, France
[2]CNRS, IN2P3, CENBG, UMR 5797, F-33170 Gradignan, France
[3] Department of Medical Physics, Royal Adelaide Hospital, Adelaide, SA, Australia
[4]School of Physical Sciences, University of Adelaide, Adelaide, SA, Australia
[5]Centre for Medical Radiation Physics, University of Wollongong, NSW, Australia
[6]Illawarra Health and Medical Research Institute, University of Wollongong, NSW, Australia
[7]International Centre for Allied Health Evidence, University of South Australia, Adelaide, SA, Australia
[8]Sansom Institute for Health Research, University of South Australia, Adelaide, SA, Australia

Keywords: Geant4-DNA, radiation, Monte Carlo method, nanoscale simulations

Corresponding Author: Eva Bezak

Address: School of Health Sciences, University of South Australia
City East Campus
GPO Box 2471
Adelaide SA 5001
Australia
Email: eva.bezak@unisa.edu.au

Abstract

Emerging radiotherapy treatments including targeted particle therapy, hadron therapy or radiosensitisation of cells by high-Z nanoparticles demand the theoretical determination of radiation track structure at the nanoscale. This is essential in order to evaluate radiation damage at the cellular and DNA level. Since 2007, Geant4 offers physics models to describe particle interactions in liquid water at the nanometre level through the Geant4-DNA Package. This package currently provides a complete set of models describing the event-by-event electromagnetic interactions of particles with liquid water, as well as developments for the modelling of water radiolysis.

Since its release, Geant4-DNA has been adopted as an investigational tool in kV and MV external beam radiotherapy, hadron therapies using protons and heavy ions, targeted therapies and radiobiology studies. It has been benchmarked with respect to other track structure Monte Carlo codes and, where available, against reference experimental measurements.

While Geant4-DNA physics models and radiolysis modelling functionalities have already been described in detail in the literature, this review paper summarises and discusses a selection of representative papers with the aim of providing an overview of a) geometrical descriptions of biological targets down to the DNA size, and b) the full spectrum of current micro- and nano-scale applications of Geant4-DNA.

1. Introduction

Mathematical and computational models describing the complex biophysical processes associated with radiation induced cell death have been used since the early 1960s. In 1973 Chadwick [1] first presented a mathematical formula which accurately fitted experimental data of cell survival as a function of absorbed dose. It was the first model that attempted to consolidate theories of macroscopic dose deposition and micro/nanoscopic damages caused by ionising radiation. In macroscopic radiobiological models (such as Chadwick's), small scale behaviour is consolidated into a set of analytical equations representing the large scale behaviour of the system. While these models are fast in terms of computation time, they are not robust enough to predict outcomes for a wide range of input parameters. As physical, chemical and biological interactions of radiation within an organic medium are stochastic processes, a stochastic type model is required for a more accurate description. As a result, with improvements to the speed and general availability of computer hardware, a transition is occurring from simple analytical models to more physically realistic stochastic (i.e. Monte Carlo) models.

In Monte Carlo codes based on a condensed history approach [2], such as EGS [3], PENELOPE [4], GEANT4 [5-7] and MCNP [8], a large number of collision processes are grouped together or "condensed" to a single "step". This approach made the Monte Carlo simulation of charged particle transport computationally feasible, but it is intrinsically inadequate to describe particle interactions at the nanometre scale. For more than twenty years the ab-initio physical mechanism at the basis of radiation damage in biological molecules has been investigated at the DNA and cellular level by means of other dedicated Monte Carlo codes, referred to as track structure codes.

A variety of track structure codes, such as PTra [9], PARTRAC [10], KURBUC [11], TRAX [12], RITRACKS [13] have been developed to calculate the energy deposition at the nanometre scale, modelling particle tracks interaction-by-interaction ("event-by-event"), typically in gaseous medium or liquid water, to approximate biological systems (this will be discussed further in section 2).

The success of the track structure codes resulted from insights from the observation that the micro and nano scale pattern of radiation track and associated energy deposition has a crucial role in the determination of the probability of formation of critical biological lesions [14]. The importance of modelling the electron interactions down to eV energies with nanoscale resolution was shown by Nikjoo and Goodhead [15]. These authors estimated that approximately 50% of all ionisations are produced by electrons with energy less than 1 keV in the case of irradiation with a photon or a proton beam. These observations have a significant impact in both radiation protection and radiotherapy studies.

More recently, emerging radiotherapy treatments demand theoretical determination of radiation track structure at the nanoscale, and the radiation damage at the cellular and DNA level. For example, in Targeted Particle (alpha, beta, Auger) Therapy, the calculation of energy deposition at cellular level is necessary because of the short path length of particles emitted by the radionuclide and the spatial distribution of the radionuclide relative to the small target volumes [16, 17]. The investigation of high-Z nanoparticles (NP) as radiosensitisers has demonstrated the need to investigate the effect of radiation at nanoscale [18]. The Local Effect Model (LEM) calculates the survival of cells exposed to a carbon ion beam based on the assumption that the cell response to a given microscopic dose deposited

by densely ionising radiation, such as carbon ions, is related to how the cell would respond to a uniform dose of sparsely ionising radiation, such as X-rays, in a particular nanoscale domain. The LEM is used clinically in the carbon ion beam Treatment Planning System at the Heidelberg Heavy Ion Therapy centre [19]. Alternatively, at the Heavy Ion Medical Accelerator (HIMAC) of NIRS in Chiba, Japan, the RBE_{10} (RBE at 10% cell surviving fraction in Human Salivary Gland tumour cells [20] was evaluated by means of the Microdosimetric Kinetic Model (MKM), formulated by Hawkins [21, 22] which is based on microdosimetric measurements.

Since its first release in 2007, the Geant4-DNA Package has been increasingly used for track structure studies. The Geant4-DNA project, originally initiated by the European Space Agency to study the effect of radiation in astronauts, was increasingly applied to other application domains.

Figure 1 shows the number of published journal articles using Geant4-DNA as an investigation tool between 2010 and 2015. As far as the authors of this paper are aware, the total number of journal articles published in this period is approximately 70. The bibliographic research was performed by means of the Scopus (www.scopus.com) database.

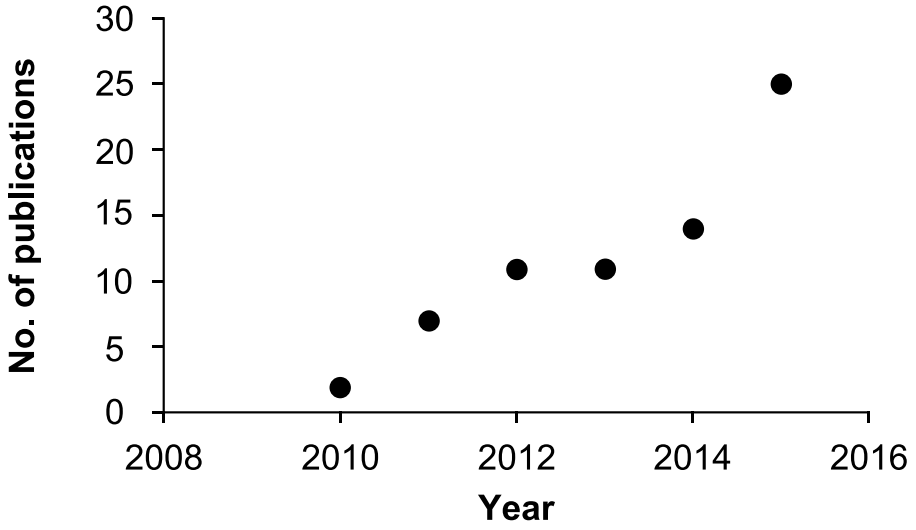

Figure 1. Number of journal articles published in the period between 2010-2015, using Geant4-DNA as an investigation tool according to Scopus database.

Given the large number of papers published, this review paper summarises and discusses a selection of representative papers with the aim of providing an overview of a) geometrical descriptions of biological targets down to the DNA size, and b) the full spectrum of current applications of Geant4-DNA.

2. Overview of physics and radiolysis modelling capabilities

2.1 Track structure codes

Track structure codes have been used for several decades in order to simulate mechanistically the physical interactions of ionising particles with biological matter at small scale and low energy. Some codes are limited to the simulation of physical interactions, while other include the simulation of water radiolysis, realistic geometrical descriptions of biological targets as well as biological repair processes. A detailed and exhaustive review as well as the inter comparison of all past and existing track structure codes is out of the scope of the current work. However, we provide a list of recent reviews on the subject, which the reader can consult; these reviews illustrate the intense on-going development activities and underline the need for such codes. The 2006 review by Nikjoo et al. [23] provides a description of suitable codes for biophysical modelling at molecular level, including full references: these are CPA100, DELTA, ETRACK, KURBUC, LEEPS, LEPHIST, LEAHIST, MC4, NOTRE DAME, OREC, PARTRAC, PITS04, PITS99, SHERBROOKE, STBRGEN, TRION and TRACEL. More recently El Naqa et al. published a topical review on Monte Carlo role in radiobiological modelling of radiotherapy outcomes [24], selecting the representative cases of the KURBUC, NOREC, PARTRAC and Geant4-DNA codes. Palmans et al. included in their recent work [25] a comparison of different Monte Carlo codes for the calculation of microdosimetric spectra (not limited to track structure codes), adding in particular a description of the PTRAN and TRAX codes. Let us finally also add to this list of codes the LQD code [26, 27], NASIC [28], PTra [9] and the RETRACKS/RITRACKS codes [29, 30].

2.2 Physics modelling

Since 2007, Geant4-DNA offers physics processes and models able to describe particle interactions in liquid water at nanometre scale [31-33]. This Package currently provides a complete set of models describing the event-by-event electromagnetic interactions of particles (electrons, protons and neutral hydrogen atoms, alpha particles including their charge states) with liquid water (as well as ionisation for a few ions – Li, Be, B, C, N, O, Si and Fe).

In brief, electron processes include ionisation, electronic excitation, elastic scattering, vibrational excitation and molecular attachment. Inelastic interactions (ionisation, electronic excitation) are derived from the model of the dielectric response function of liquid water developed by Emfietzogou, as recently recalled in [34]. In the most recent Geant4 release (10.2), a new improved implementation of this model has been added in order to account for binding-energy thresholds through a re-distribution of the oscillator strength and refinements in the exchange and perturbation corrections to the Born approximation, as described in detail in [35]. Three elastic scattering models are provided, either derived from a full partial wave analysis for the liquid phase, or from the analytical Screened Rutherford theory with a low energy screening parameter derived from data either in nitrogen gas or in gaseous water [31]. Finally, regarding sub-excitation electrons, vibrational excitation is based on the Michaud et al. measurements scaled for the liquid phase, and molecular attachement based on experiments by Melton [36].

Interactions of protons, neutral hydrogen, neutral helium and charge states take into account ionisation, electronic excitation, electron loss or capture and elastic scattering; the corresponding models are described in detail in [32] and in all references cited therein. Low energy ionisation for protons is described using the semi-empirical approach proposed by Rudd et al. (<500 keV) and it is based on the dielectric formalism above this energy, as proposed by Dingfelder et al. [37]. Low energy excitation for protons and neutral hydrogen

uses a speed scaling from electrons proposed by Miller and Green (< 500 keV) and it is based on the Born and Bethe theory above this energy (for protons only). Electron loss and capture follow the semi-empirical approach also proposed in the work by Dingfelder et al. Finally, elastic scattering is modelled from a classical approach presented recently in [38]. These approaches are also used for the description of ionisation (semi-empirical model by Rudd et al.) and electronic excitation (speed scaling approach from protons by Miller and Green) by helium atoms and their charge states. Electron loss and capture follow the semi-empirical approach of Dingfelder et al. presented in [39]. Elastic scattering is modelled usign the same method as for protons.

Finally, regarding ions heavier than helium, only ionisation is currently modeled, above about 1 MeV/amu, based on the Rudd approach and including relativistic extension and considering the effective charge of the ion [40].

The inclusion of new and/or alternative physics models in Geant4-DNA for liquid water or other target materials remains fully open, especially if developers of the above listed track structure codes are interested in providing their models in open access to the community.

2.3 Water radiolysis modelling

Since Geant4 release 10.1, Geant4-DNA includes models of free radical production, diffusion and chemical reactions, following the physical stage of interactions of particles with liquid water. Such functionalities allow the simulation of water radiolysis up to one microsecond after irradiation. These developments are described in detail in the recent papers by Karamitros et al. [41, 42], which include comparisons of Geant4-DNA simulated radiochemical yields to simulation and experimental literature data. They will be required for the simulation of indirect effects of ionising radiation to DNA. Such effects are known to be dominant especially in the low LET domain (see for example Hirayama et al. [43]).

Key parameters are based on PARTRAC as further explained in [41, 42]. In particular, the dissociation scheme is presented in Table 2 of ref. [31], starting from ionised or excited water molecules or dissociative attachment, simulated using the physics models previously presented. The list of molecular species currently considered in the simulation of water radiolysis is as follows: H_3O^+, OH^-, •OH, H•, H_2, e^-_{aq}, H_2O_2. Their diffusion coefficients are listed in Table 1 and reaction and reactions rates are given in Table 2.

Table 1: list of available molecular species and corresponding diffusion coefficients.

Species	Diffusion coefficient (10^{-9} m^2 s^{-1})
e^-_{aq}	4.9
•OH	2.8
H•	7.0
H_3O^+	9.0
H_2	5.0
OH^-	5.0
H_2O_2	1.4

Table 2: list of reactions and reaction rates.

Reaction	Reaction rate (10^7 m^3 mol^{-1} s^{-1})
$H_3O^+ + OH^- \rightarrow 2\ H_2O$	14.3
$\bullet OH + e^-_{aq} \rightarrow OH^-$	2.95
$H\bullet + e^-_{aq} + H_2O \rightarrow OH^- + H_2$	2.65
$H_3O^+ + e^-_{aq} \rightarrow H\bullet + H_2O$	2.11
$H\bullet + \bullet OH \rightarrow H_2O$	1.44
$H_2O_2 + e^-_{aq} \rightarrow OH^- + \bullet OH$	1.41
$H\bullet + H\bullet \rightarrow H_2$	1.20
$e^-_{aq} + e^-_{aq} + 2H_2O \rightarrow 2OH^- + H_2$	0.50
$\bullet OH + \bullet OH \rightarrow H_2O_2$	0.44

The following section will concentrate exclusively on Geant4 user applications adopting Geant4-DNA physics processes only, as research based on Geant4-DNA water radiolysis is not published yet. We briefly introduce in the last section of this paper two applications involving Geant4-DNA radiolysis simulation, one for validation purpose and the other one for nanoparticle sensitization study.

3. Geometrical models of DNA

One of the main goals of the Geant4-DNA Package is to be able to predict early damage to DNA [31, 44], taking into account both direct and indirect deleterious actions of ionising radiation on sensitive biological targets. In order to simulate damage to DNA, Geant4-DNA can be utilized following three approaches: (1) the estimation of damage using clustering algorithms, (2) the explicit geometrical modelling of the DNA double helix and associated biological structures of interest, and (3) a mixed approach combining the usage of clustering algorithms with geometrical modelling. These three approaches are described in the following paragraphs.

3.1 Clustering algorithms

The first approach consists of analysing the pattern of energy deposition in the irradiated medium using a clustering algorithm that is tuned in order to reproduce experimental data, e. g. on DNA strand break yields (single strand breaks (SSB), double strand breaks (DSB), complex strand breaks) and survival rates. Francis et al. [40, 45, 46] were the first to propose such an approach based on an adaption of the DBSCAN algorithm [47]. They could simulate SSB, DSB and DSB/SSB ratios as a function of incident proton energy close to other simulated and experimental data on cells and plasmids obtained from the literature. While their algorithm was not included in Geant4/Geant4-DNA, Perrot et al. followed a similar approach as Francis et al., adapting the algorithm from DBSCAN, and they included this clustering algorithm in the “clustering” Geant4-DNA “extended” example in December 2015 (Geant4 release 10.2), and is described in more detail in [31]. They could predict DSB/SSB ratios as a function of incident proton energy close to values predicted by the PARTRAC code [10] and reproduce the results by Francis et al.[46]. The "clustering" example can be conveniently controlled using Geant4 user interface and includes user commands for the

setting of clustering parameters, such as the minimum number interaction points (located in space and associated to a local energy deposition) to form a cluster, the probability that a point falls within a sensitive region of a target, the maximum distance separating two points in a cluster and the probability to induce a strand break. Once clusters have been formed, the code scans all clusters once and merge them if their barycenters are separated by less than the maximum distance selected by the user (this is a simplification compared to the DBSCAN algorithm and to the code developed by Francis et al.). The code can also be used with the most recent Geant4-DNA physics models (see section 2), and it calculates single, complex single and double strand breaks as well as cluster sizes and its performance is illustrated in Bernal et al. [31].

Douglass et al. [48] also proposed independently their own clustering code, allowing in particular the simulation of V79 cell survival after irradiation with MeV protons. The algorithm is based on a hierarchical, geometric clustering process which attempts to group closely spaced ionisation events into DSBs. This code is currently not available in Geant4-DNA. While this approach is interesting for immediate applications (see e.g. [49]), it currently does not take into account the mechanistic simulation of physico-chemical and chemical interactions with sensitive biological targets, which may be required for detailed simulations of damage induction.

3.2 Geometrical approach

Alternatively, another approach consists of developing geometrical models of biological targets that can be combined with the simulation of physical, physico-chemical, chemical and biological processes in order to mechanistically simulate damage, such as DNA strand breaks and base oxidation. In the last four years, significant progress has been made in this direction using Geant4-DNA. Two main categories of geometrical models of DNA have been developed for the prediction of damage to DNA: (a) a cylindrical approach where sensitive volumes are described using combinations of elementary cylinder volumes, and (b) a high-resolution atomistic approach were component atoms are represented individually. These geometric models are described below.

The cylinder volumes approach

Bernal et al. [50] proposed the first combination of Geant4-DNA physics modelling in liquid water with a geometrical description of DNA based on previous simulations performed with the PENELOPE Monte Carlo code [51, 52]. The DNA double helix is represented as a series of slices in the B-DNA conformation, each of them including two phosphodiester groups bound by a complementary base pair (bp). The base pairs are represented by cylindrical shells and each slice is rotated from its neighbour in order to build a full double helix loop of 100 bp. Nucleosomes are modelled as cylindrical histones surrounded by two DNA loops and they are assembled into 30-nm chromatin fibres, each containing a total of 3600 DNA bp. Irradiating a total of 900 fragments of such chromatin fibres with incident protons and alpha particles in the 0.5 – 10 MeV range, the authors could demonstrate that the total strand break yield and the number of energy deposition events required to reach a certain absorbed dose were found nearly independent of the type and energy of the incident ion. The SSB generation process was found to be homogeneous, depending neither on the structure of the DNA nor on the LET of the particles involved, while the DSB yield was found strongly dependent on the LET of the incident radiation [50].

Using the same geometrical description of DNA, Incerti et al. [53] proposed to construct directly in a Geant4 application a simplified nucleus made of randomly oriented short segments of chromatin fibres, for a total of 6×10^9 bp. This simplified nucleus was irradiated with incident protons and the authors confirmed the weak dependence of the total strand break yields with incident particle LET, as already observed in [50]. The DSB yield was found to be strongly dependent on LET. These yields were also found to depend strongly on the method used to account for a direct SSB when compared to other simulated or experimental data.

The B-DNA geometrical model was further completed with two other models, describing the A- and Z- conformations of DNA [44]. It was found by the authors that the total direct strand break yield for a given DNA form depends weakly on DNA conformation topology and this yield is practically determined by the target volume of the DNA configuration. On the contrary, the DSB yield was found to increase with the packing ratio of the DNA double helix, and thus dependent on the DNA conformation.

This cylindrical approach was also followed by Semsarha and colleagues for the prediction of DNA damage in a variety of studies: from Auger emitter radionuclides (^{123}I and ^{125}I) [54], from ^{60}Co gamma rays [55, 56] and from ultrasoft X-rays [57].

Their study on iodine isotopes used two geometrical implementations of 41 base pairs in the B-DNA conformation, the first being similar to the one proposed by Bernal et al. [50], the second having a finer granularity. For the first time with Geant4-DNA, they also included a method using a liquid water virtual cylinder around the DNA for the recording of indirect effects, initially proposed by Pomplun [58] and using prototype radiolysis simulation capabilities available in Geant4-DNA. The authors demonstrated the reasonable agreement on the number of strand breaks per radionuclide decay between Geant4-DNA and theoretical and experimental works from the literature, underlining the applicability of Geant4-DNA for nanodosimetry. They also recommended the usage of accurate geometrical representations of DNA for reliable predictions of indirect effects [54].

The same groups performed two studies on DNA irradiation from ^{60}Co gamma rays. The first study investigated the influence of DNA conformation of strand break yields [55]. The three B-, A- and Z-DNA conformations were studied for 34 bp segments of DNA, including the B-DNA description based on the earlier work by Charlton and Humm [59]. They also took into account a liquid water hydration shell around the DNA for the recording of both direct and indirect effects. From their simulations, the authors observed variations in strand break yields compared to other experimental or simulation works for B-DNA (23% at maximum). They concluded that the B-DNA conformation, the most common conformation of DNA in cells, has the lowest sensitivity for both types of strand break damage. The A-DNA has the highest SSB yields and the Z-DNA has the highest DSB yields. The second study on ^{60}Co gamma rays irradiation focused exclusively on direct effects in a total of about 105 bp [56]. The authors investigated direct strand breaking for several organization levels of DNA: double helix, beads-on-a-string, solenoid (with and without histone proteins) and chromatin loop, starting from the B-DNA geometrical model in [52]. An illustration of a 300 nm chromatin fibre loop is shown in Figure 2, taken from [56]. They found reasonable agreement for DSB yields compared to other theoretical and experimental works, but significant differences for SSB yields of up to 68%. They suggested that the direct strand breaks yields depend mainly on the primary double helix structure of the DNA and that the higher-order structures do not

have a noticeable effect on the direct DNA damage under ^{60}Co gamma rays irradiation. The influence of histones on strand break induction was found to be negligible, while the dependence with DNA structure volume was underlined.

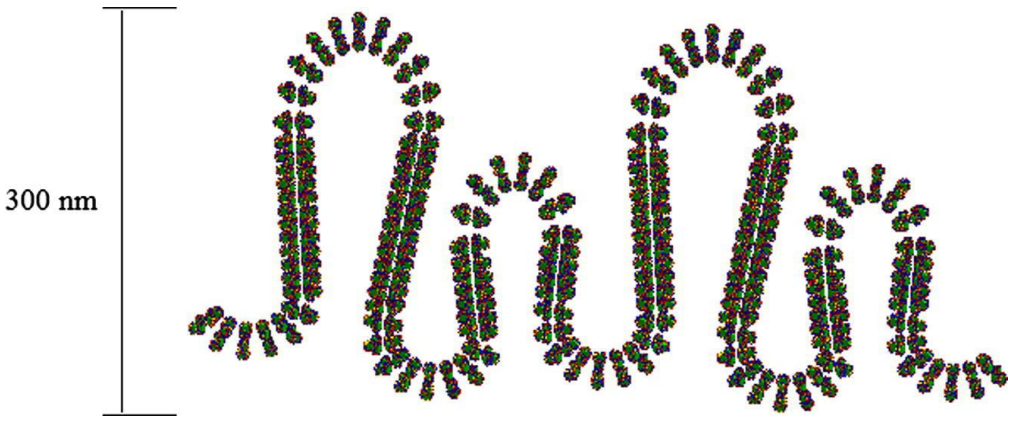

Figure 2. Example of 300 nm chromatin fibre loop implemented in Geant4 (Courtesy [56]).

Finally, this group also investigated damage induction from ultrasoft X-rays. They used the Charlton and Humm model [59] for the calculation of direct and indirect damage, for a total of about 10^6 bp. They obtained predictions similar to theoretical and experimental works demonstrating the efficiency of this simple approach. They observed a direct dependence of DSB induction, relative biological effectiveness (RBE) for the induction of DSB and mean lineal energy in strands, connecting nanodosimetry and microdosimetry observations. They also underlined the influence of the SSB threshold induction on break yields, suggesting a value of 10.79 eV for the first ionisation threshold in Geant4-DNA default models.

A last study based on a similar geometrical approach has been proposed by Li et al. [60]: the geometrical model by Charlton and Humm [59] has been used in combination with six different sets of inelastic cross section data describing the transport of electrons and calculated by the authors. These data were imported into their own Geant4-DNA application. These cross sections data were based on Emfietzoglou's approach, as Geant4-DNA models, but included two different optical datasets (by Heller or Hayashi) and three different dispersion models (the extended-Drude model, the extended-oscillator-Drude model and Ashley's delta-oscillator model). Further details on these cross section data are given in [60]. The geometrical model allowed the authors to demonstrate that the six inelastic cross sections have a notable influence on the direct DNA strand break yields, underlining again the necessity of accurate physics models for the simulation of electron physical interactions in liquid water.

The high-resolution atomistic approach

The works described in the previous paragraph (e.g. [54]) have underlined the influence of DNA conformation on indirect damage yields induced by chemical species on DNA critical sites. Bernal et al. recently proposed the first freely available stand-alone subroutine allowing the construction of a fully atomistic geometrical description of B-DNA [61]. In this model, the authors accounted for five-organization levels of the DNA, from the nucleotide pair up to the 30 nm chromatin fibre. The provided subroutine is also capable of calculating the distance from an arbitrary point in space to the closest atom, a requirement when one needs to

calculate if a given energy deposition is located in a target volume of interest. This subroutine is not available in Geant4-DNA but can be downloaded as described in [61]. This atomistic model was then used in combination with Geant4-DNA physics modelling capabilities in order to compute direct strand breaks [62]. The authors implemented a cell nucleus containing about 6.5×10^9 base pairs; all atoms were explicitly represented as spheres with corresponding Van der Waals radii. Damages were calculated for incident proton and alpha particles, in the 0.5 – 10 MeV incident energy range. Total damage yields for protons were found consistent with predictions by the PARTRAC software which also uses an atomistic approach [63]. For alpha particles, SSB yields were close to experimental measurements, while DSBs yields appeared larger than experimental values.

In parallel, Xie et al. [64] compared estimations obtained using the previously described cylinder volume approach (model from Charlton and Humm [59]) with an atomistic model created from published DNA atomic coordinates; they also studied the effect of doubling Van der Waals radii in the atomistic model in order to take into account DNA hydration shell. In their results, the authors extracted simple and complex damage yields and demonstrated that the yields obtained with the cylinder volume approach were the highest. They underlined the necessity to take into account complex DSB damage. No comparisons to other calculations or measurements were presented.

A promising approach has been recently included in Geant4-DNA, allowing the implementation of atomistic geometries of a large variety of macromolecules, directly from the Protein Data Bank© (http://www.rcsb.org). This is described in the work of Delage et al. [65] (http://pdb4dna.in2p3.fr) who developed a dedicated Geant4-DNA extended example, the so-called "pdb4dna" example. This example also includes a cross-platform C++ library of tools. With this code, users can easily implement macromolecules geometries available in the Protein Data Bank© directly in their Geant4 application. In the case of DNA, the granularity of the geometrical model can be selected easily at three levels: representation of individual nucleotides, or representation of components of nucleotides (sugar, phosphate, base) or representation of each individual atom for a full atomistic description (see Figure 3). An algorithm capable of finding the closest atom to an energy deposition is also included, as well as computation of DNA strand breaks.

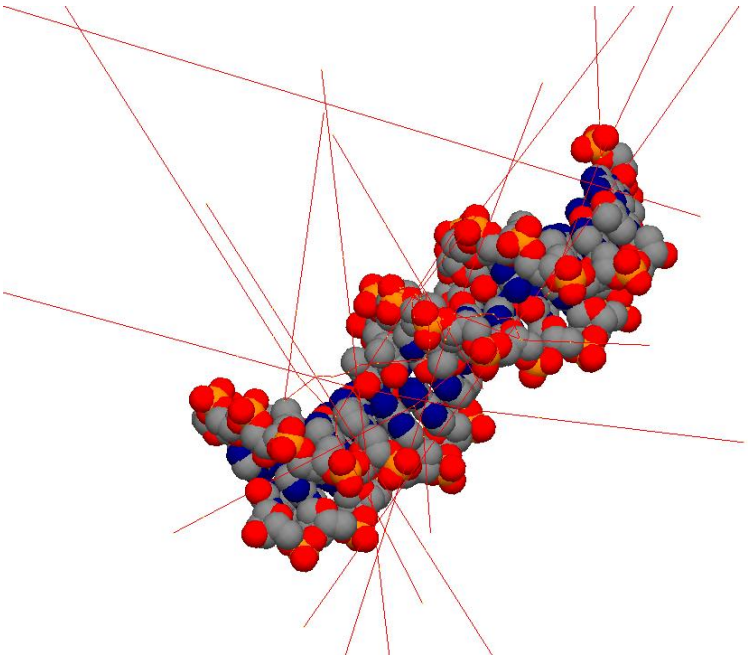

Figure 3. Example of irradiation of the 3BSE 16-base-pair B-DNA PDB© molecule by 10 incident 10 keV electrons, simulated with the Geant4-DNA "pdb4dna" example [65].

The combination of such an atomistic approach with the simulation of radiolysis will be required in order to simulate indirect damage accurately; such a feature is currently under development and is expected to be released in the near future in Geant4-DNA [31, 66].

The mixed approach

In parallel to the previously described applications, a mixed approach has been proposed by Dos Santos and colleagues from 2013 using Geant4-DNA [67-71].

They first proposed the geometrical implementation of two nuclei (including $6x10^9$ bp) for a fibroblast and an endothelium cell in the G0/G1 phase. The fibroblast nucleus is included in Geant4-DNA as the so-called "wholeNuclearDNA" extended example [31]. They included five compaction levels: the DNA double helix, nucleosomes, chromatin fibres, chromatin fibre loops and chromosome territories. The reader is invited to look at illustrations available in the recent work of Bernal et al. [31]. In order to simulate direct damage from proton irradiation (0.5 – 50 MeV range), they applied the adapted DBSCAN [46, 71] clustering algorithm to energy deposition events simulated with Geant4-DNA physics processes and located in the sugar-phosphate group. The clustering algorithm is used for the estimation of potential SSBs and DSBs. With this study, the authors could underline the dependence of the quantity and complexity of clusters with increasing DNA density, as in endothelium cells. They extended this work to alpha particles (5 – 50 MeV range) [70] and confirmed that the quantity and the complexity of the potential direct damages in the endothelium cell nucleus are always higher than in the fibroblast cell nucleus. In addition, both studies showed that for a given LET, a proton irradiation induces more direct complex clustered damages than an alpha particle irradiation.

Using a similar approach, they also investigated the influence of chromatin condensation on direct DSBs induced by incident protons and alpha particles by comparing two types of chromosome territories corresponding to euchromatin (decondensed) or heterochromatin (condensed) regions [69, 70]. They reported that condensed chromatin could be the location of more severe radiation-induced lesions than decondensed chromatin.

The same group recently proposed to investigate the influence of the geometrical description of DNA on nanodosimetry parameters of track structures under proton an alpha particle irradiation (in the 1 to 162.5 keV/µm LET range) [67, 68]. Geant4-DNA simulations were performed in a cylindrical target volume (equivalent to 18 kbp of DNA) containing either the previously described detailed implementation of the double helix [71] or randomly oriented 10-bp long individual homogeneous cylinders as in [72], an approach commonly used in experimental nanodosimetry. Counting ionisations in scoring volumes and using their adapted DBSCAN algorithm in the detailed implementation of the double helix, they could compare the topology of ionisation clusters in both geometries using several nanodosimetric quantities. From their simulations, the authors recommended the usage of the detailed DNA geometry and a scoring method without fixed boundaries in order to extract biologically relevant ionisation cluster size distributions [67, 68].

There is thus a large variety of works, which are proposing different geometrical approaches for the modelling of DNA damage using Geant4-DNA. These studies suggest the need for detailed geometrical models of DNA, which shall ultimately be used for the scoring of both direct and indirect damage. In parallel, the recent development of experimental detection of DNA repair proteins using fluorescence time lapse imaging [73, 74] will provide unique opportunities to validate such simulations over different time scales. This will be needed particularly for the inclusion of repair processes in Geant4-DNA, allowing damage estimation well beyond the microsecond, the maximum time limit reachable by the simulation of water radiolysis in Geant4-DNA.

4. Geant4-DNA applications in radiation therapies

Since 2010, Geant4-DNA has been adopted as investigation tool a) in external beam radiotherapy using megavoltage photons produced in medical linear accelerators, b) in hadron therapies using high-energy protons and heavy ions, c) for the study of radiosensitisation in radiotherapy using NPs and d) in targeted therapies where tumour cells are directly targeted by a vector with a radioactive substance attached, including targeted alpha or beta therapy and Auger electron therapy. Some of these studies made use of the geometrical models summarized in the previous section. We present below an overview of these applications in radiation therapies.

4.1 X-ray radiation therapy

Conventional radiation therapy

For radiation therapy purposes, the interaction of radiation is often modelled in water medium. However, there has been a trend to model semi-realistic cell media representing tumours as well as healthy tissue. In the past, simplified spheroid models with different cell and nucleus radii were used to model cells [75]. Recently, some more realistic cell and tumour models were built [76-78]. Most of the works published to-date have modelled X-rays, gamma-rays and low energy electrons and have investigated production of SSBs and DSBs in order to evaluate the efficacy of various radiation therapy modalities.

For example, in the previously described study of Tajik et al. [57] the total yields of SSB and DSB induced by monoenergetic electrons with energies of 0.28–4.55 keV, corresponding to ultrasoft X-rays energies, have been modelled in the Charlton and Humm volume model using the Geant4-DNA toolkit. They observed that in the low energy region, the yield of SSBs remained fairly constant while the yield of DSBs increased with decreasing energy. Moreover, a direct dependency between DSB induction, RBE value and the mean lineal energy as a microdosimetry quantity was noticed.

In the other study of Tajik et al. [56], ^{60}Co irradiation was modelled using Geant4-DNA. The yields of direct SSBs and direct DSBs yields induced by secondary electrons were obtained for several DNA modelling structures. As the results obtained agreed well with the experimental data, the authors concluded that Geant4-DNA is a useful tool for micro and nano dosimetry calculations at cellular and sub-cellular levels. They also investigated the importance of modelling the primary (i.e. photon) and secondary (i.e. electron) radiation spectra. They concluded that the DSB yield depended primarily on the secondary electrons

and similar yields were obtained whether the primary photons were modelled or not. The SSB yields, however, decreased if only secondary electrons were considered.

Microbeam Radiation Therapy (MRT)

Geant4-DNA has also been adopted to characterise the secondary electron track structures for 30, 50 and 100 keV X-ray microbeams of width 20 μm, in a water phantom, in a first attempt to get an insight into the physical mechanism at the basis of MRT [79, 80]. The two studies demonstrate the importance of simulating track structures at nanoscale level to more realistically capture the full extent of radiation damage, while dose alone is inadequate for describing radiobiological effectiveness.

The study by McNamara et al. [81] compared the track structures of therapeutic MRT X-ray and proton beams in the attempt to find similarities between the two. If it can be shown that the ionisation cluster distributions are similar, the substitution or supplementation of photon microbeams for protons in targeted single cell irradiations could be feasible. The results of this study suggest that low energy X-rays could produce similar ionisation cluster distributions to MeV protons on the DNA scale at depths greater than ∼10 μm and at distances greater than ∼1 μm from the beam centre.

4.2 Hadron radiation therapy

Hadron therapy encompasses irradiations with neutrons, pions, protons and light ions such as carbon ions. Nowadays, proton therapy and carbon ion therapy are the most prevalent forms of hadron therapy and this section will focus on the Geant4-DNA applications to these particle beams.

While the sharpness of the Bragg peak is an important advantage of light ion beams for treatment conformality to the tumour, the rapidly changing stopping power at the end of the particle range means that the energy deposition characteristics of the beam also change with depth. LET increases with an associated increase in ionisation track structure density in the region of the Bragg peak. Quantifying the biological effect of this change in track structure has been the subject of a number of studies (see, for example, [82, 83]). In current clinical practice, the RBE of proton therapy is assumed to be a constant value of 1.1. This value is a result of experimental studies and clinical outcomes [84]. However, it is known that RBE is a complex quantity that depends on dose, LET, cell type, surrounding tissues, biological endpoint and other factors.

Radiobiological effects are handled somewhat differently in carbon ion therapy, where the varying RBE along the Bragg peak is accounted for with an LET-based radiobiological model. A non-uniform physical dose is delivered in an attempt to deliver a uniform RBE weighted dose [85]. Considering the importance of LET and ionisation track structure in hadron therapy treatment planning, a thorough understanding of the physical and radiobiological properties of irradiation by these beams is crucial.

Verification and validation of Geant4-DNA for hadron therapy applications

Several investigations have reported on the validity of the ionisation track structure calculated by Geant4-DNA for incident hadrons. Bug et al. [86] compared the Geant4-DNA angle-

dependent energy spectra of secondary electrons created by proton irradiation of amorphous solid water with measurements performed by Toburen et al. [87]. The authors found that simulated spectra were in good agreement with the measured spectra for electron energies between 50 and 100 eV. Above 100 eV measured electron yields were underestimated by Geant4-DNA by approximately 60%. The authors suggested this may have originated from the abrupt limit of the low-energy excitation cross-section at this energy. Below 50 eV, Geant4-DNA increasingly overestimated the yield of electrons, reaching a factor of 7 at 2 eV. However, the authors demonstrated that inclusion of a potential step to model the surface barrier potential of water improved the agreement of simulated and measured yield of electrons below 50 eV, reducing the discrepancy to a factor of 3.

Wang and Vassiliev [88] utilized Geant4-DNA to validate radial dose distributions along single particle tracks for application in the Amorphous Track Model (ATM) commonly applied in RBE models in hadron therapy. The ATM and its variations, including the Local Effect Model, rely on a simplified model of a heavy charged particle track with a track structure characterized by the radial dose distribution from the primary particle [89]. Wang and Vassiliev compared Geant4-DNA calculated radial dose distributions with analytical calculations for proton energies between 10 MeV and 100 MeV. The authors demonstrated that their newly proposed formula could better match the Geant4-DNA radial dose distribution than existing formulae.

Francis et al. [90] compared stopping powers and ranges of electrons, protons and alpha particles in liquid water with analytical models and ICRU data. They found that Geant4-DNA resulted in lower proton stopping powers than ICRU 49 [91] below 10 keV and correspondingly larger particle ranges below 100 keV, but were in good agreement above these energies. This was further improved by including the elastic scattering process in simulations [38]. Nanometric proton energy deposits calculated with Geant4-DNA with the TRIOL code and experiments of Borak et al. [92] were also conducted by Francis et al. [36]. In addition, Francis et al. [40] also presented a Geant4-DNA study of energy depositions due to protons, alpha particles and carbon ions of the same LET in liquid water. Energy deposition spatial distributions were analysed using an adapted version of the DBSCAN clustering algorithm [46]. The calculated yields of clustered and single damage and their ratios were directly compared with experimental data on SSB and DSB obtained by the gel electrophoresis technique on irradiated plasmid DNA and other DNA types. The simulation showed good agreement with the experiments and also with the results obtained by the PARTRAC calculations for protons.

While the works mentioned above were all based on the irradiation of water, Champion et al. extended the work of proton irradiations with Geant4-DNA in water to simulations in DNA nucleobases [93, 94]. The authors concluded that material selection had a non-negligible effect on energy deposit distributions in nanometre size targets of constant density. The findings bring into question the validity of simulating biological systems as uniform water environments.

Hadron therapy applications of Geant4-DNA

Pham et al. [95] compared measured and simulated depth-dose distributions for therapeutic proton beams when the Geant4-DNA Package was incorporated into the GATE [96] toolkit. The authors also evaluated frequencies of energy depositions and DNA damage in the simulated proton beams. DNA damage was evaluated using an algorithm to allocate energy

depositions to atoms constituting DNA molecules represented by their Protein Data Bank (PDB) description. The PDB format provides a standard representation for macromolecular structure data obtained from X-ray diffraction and NMR studies. Proton and electron ranges were calculated with Geant4-DNA implemented in GATE v7.0. No significant differences were observed, validating the porting of Geant4-DNA physics models in GATE. The authors also compared the calculated ranges with ICRU published data and found good agreement with relative differences of less than 8.5% for proton energies between 100 keV and 100 MeV and less than 4.8% for electron energies between 10 keV and 100 keV. This work provided an example of merging the popular macroscopic dosimetry toolkit GATE with sub-cellular track structure modelling of Geant4-DNA.

Francis et al. [97] utilised Geant4-DNA to examine the track structure of therapeutic carbon ion beams in the fragmentation region distal to the Bragg peak. The authors concluded that the energy deposition clustering yields per event in the fragmentation region were approximately three times less than those induced by the 400 MeV/amu carbon beam within a few centimetres of the phantom surface. These calculations suggest an agreement with the RBE ratio of 3 between the entrance beam and the Bragg peak tail as measured by Scholz et al. [98] in Chinese hamster ovary cells.

Casiraghi and Schulte [99] utilized Geant4-DNA to calculate nanodosimetric quantities for therapeutic proton and carbon ion beams in a simplified water environment. The nanodosimetric quantities for each pencil beam were subsequently implemented in an inverse optimization routine to generate beams of uniform nanodosimetric properties, rather than physical dose properties.

4.3 Nanoparticle radiosensitisation

In the last ten years, the study of high atomic number (Z) nanoparticles (NPs) to enhance radiotherapy treatment has been the subject of significant interest in the scientific literature, as this technique shows very promising results in radiobiological experiments. Geant4 offers the capability to select different physics models in different regions of the simulation set-up. This allows the user to select condensed-history physics models, such as the “Low Energy” or “Standard” electromagnetic categories, for modelling particle interactions in the NP, while selecting the Geant4-DNA Package for the surrounding liquid water representing the biological medium, as shown in Fig.4. A 40 MeV proton pencil beam is incident on a water phantom with size equal to 200 μm, where the Geant4-DNA processes are active. A gold nanoparticle is positioned in the centre of the water phantom. In this region the particle interactions are described by means of the Geant4 condensed-random walk scheme physics models. Fig.4 shows the energy deposition produced by the proton beam in a subregion of the water phantom, containing the NP, with a lateral size of 0.2 μm. It can be observed that the description of the proton track structure is much more refined in the liquid water medium where the Geant4-DNA Package is used.

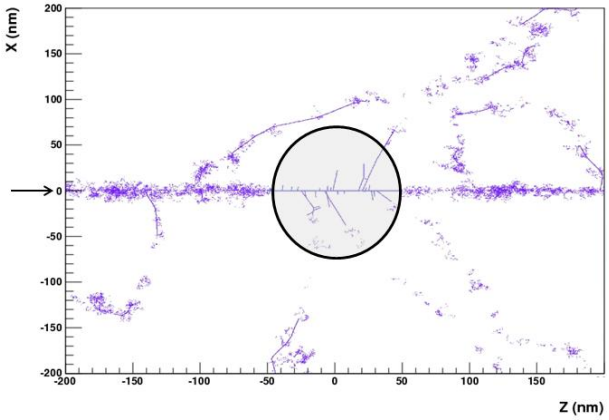

Fig. 4: Geant4-DNA simulation of a 40 MeV proton pencil beam incident on a liquid water phantom with size 200 μm. The direction of incidence of the beam is indicated by the black arrow on the left. A gold NP is placed in the water phantom (grey area enclosed by the black circle). Geant4-DNA processes are activated in the water phantom, while Geant4 condensed-history processes are used to simulate interactions in the NP. The plot shows the energy deposition topology (in arbitrary units) in a subregion of the water phantom containing the NP, with lateral size 0.2 μm. Image courtesy of S McKinnon and S Guatelli, Centre for Medical Radiation Physics, University of Wollongong [100].

McMahon et al. utilised Geant4-DNA models to simulate the dose distributions around GNPs (GNPs) on nanometre scales [18]. Geant4-DNA was selected to provide sufficient accuracy of the track structure in the water volume surrounding the GNPs. The biological effect of GNPs with diameters between 2 and 50 nm being irradiated by monoenergetic photons with energies between 20 and 150 keV was quantified using LEM. A single GNP of varying diameter (between 2 and 50 nm) was placed in the centre of a water cube of side length 200 μm and irradiated with monoenergetic photons between 20 and 150 keV. The rate at which ionisation events occurred in the gold, the spectrum of secondary electrons and the dose distribution in close proximity to the GNP surface were calculated. The study highlighted the role of Auger electrons in the enhancement of the dose close to the NP boundary. The higher energy photo or Compton electrons were found to travel long distances, depositing most of their energy away from the surface of the GNP, whereas Auger electrons deposited most of their energy in the vicinity of the GNP surface. It was also found that the dose deposited in the vicinity of the GNP following a single ionisation event in the gold was dependant on the size of the GNP. Smaller (2 nm) GNP showed the greatest dose deposition outside the NP due to its greater surface area to volume ratio. The Local Effect Model was applied to quantify the radiosensitisation effect of the GNPs. The model was applied to MDA-MB-231 breast cancer cells and it was found to agree with the cell survival curve obtained in radiobiological experiments. This study demonstrated that it is essential to take into account the dose inhomogeneities produced at nanoscale by NPs to be able to predict the experimental results obtained *in vitro* with more accuracy by means of the LEM.

Recently McMahon et al. [101] performed the first systematic study comparing the dose enhancement of alternative NP materials, spanning from silicon (Z=14) to mercury (Z=80), as possible NP contrast agents and radio sensitisers for imaging and radiotherapy applications. The Geant4-DNA Package was selected to model particle interactions in kV and MV photon beams. The purpose of the study was to investigate the underlying mechanism of

dose deposition due to ionising radiation interactions with NPs. A 20 nm diameter NP was placed in a cube of water with side lengths of 10 μm. The "Livermore" set of low energy electromagnetic physics models of Geant4 was used to simulate radiation interactions in the NP and Geant4-DNA was utilised in the surrounding water medium. NPs were spheres composed of pure elemental compositions ranging from Z=14 to Z=80 with densities and isotope distribution based on NIST reference values. Only solid elements were considered in this study (no gas or liquid phase elements). The NPs were irradiated with kV photon energies and these were set depending on the material. The energy was set to be 20 keV higher than the K-edge of the material being exposed. The energies ranged from 22 to 102 keV. The beam width was set to 20 nm so that the entire NP was exposed. NPs were also exposed to a clinical 6 MV linac spectrum. For both spectra, all secondary particles emitted from the NP were scored. The process leading to their emission was identified and the dose deposited was scored in concentric 2 nm shells around the NP out to a range of 1 μm. The LEM was then used to quantify the radiosensitisation effect. The results indicated that while photo electrons contribute most strongly to the overall dose enhancement at kV energies, the dose enhancement within 1 μm of the surface of high Z NPs is due primarily to Auger electrons. Photoelectrons have a large range which results in much of the dose being transported away from the NP. In the case of megavoltage photons, the total dose deposited is dominated by secondary electrons from Compton scatter processes. The effects of Compton electrons are mitigated due to their long range and a contribution from Auger electrons is still seen at short range but this contribution is smaller compared with kV photons.

It was concluded that there are significant variations in radiosensitisation effect for different atomic number NPs. These differences are driven mainly by differences in Auger electron spectra. At least for kV photons, material specific energy tuning is likely to be possible to account for the characteristics of secondary electron energy deposition and NP design.

Douglass et al. developed a randomised 3D tumour model in Geant4 [102, 103]. A cluster of 850 cells representing a small tumour was developed as a geometry for Geant4. The translation and rotation of the membrane of each cell was parameterised using *Geant4 Parameterised Volumes*. Each membrane geometry contained the cytoplasm, reticulum, nucleus and nucleolus. The cellular geometry was applied to investigate the radiosensitisation effect of different sized GNPs from kV and MV photon radiation. Two gold geometries were investigated; a 300 nm thick spherical shell of gold representing a cloud of NPs surrounding the nucleus and a single 400 nm diameter gold sphere in the cytoplasm (Figure 5). These geometries were selected to represent the extrema of possible internalised GNP geometries. The simulations utilised both the Geant4 "Livermore" and Geant4-DNA models. A typical clinical 80 kVp superficial and 6 MV linear accelerator energy spectrum was used to irradiate the cells.

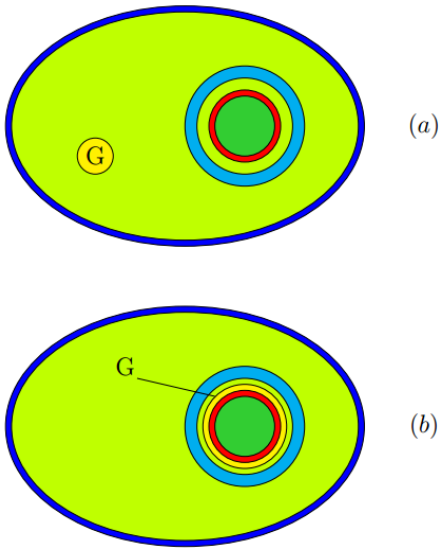

Figure 5. Illustration of cell cross-section with two types of simulation geometries. (a) 400 nm gold cluster (yellow) located randomly in the cytoplasm (lime) and (b) a thin (300 nm) layer of gold (yellow) is attached to the nucleus. Membrane: Dark Blue, Cytoplasm: lime, Reticulum: Cyan, Nucleus: Red, Nucleolus: Green, GNPs: Yellow (Courtesy [103]).

It was concluded that the largest contribution to the dose enhancement effect from GNPs was from increased photoelectron production due to a higher interaction cross section with gold at kV photon energies. It was also shown that Auger electrons may play an important role in the dose enhancement effect at small distances from the gold (up to 500 nm from the surface). Both findings were consistent with the results of McMahon et al. [18]. As a result, GNPs must be internalised close to, or inside, the nucleus in order to produce a significant dose enhancement effect.

Martínez-Rovira et al. [104] utilised GATE 7.0, to investigate the radioenhancement of gold and gadolinium NPs in proton therapy. The research aimed to investigate the effect of NP size, distance between source and NP on NP radiosensitisation. The energy deposited by a proton beam of 200 MeV incident on a NP was calculated in spherical shells around the NP. This work showed that, differently from the case of X-ray radiotherapy, the Auger electrons do not play a crucial role in the determination of the energy deposition enhancement and that the geometrical configuration of the simulation set-up plays a fundamental role when calculating the energy deposition. When adopting a more realistic set-up, the dose enhancement decreases significantly. The authors suggested that physical effects do not seem to be responsible for the NP induced proton radiosensitisation that has been shown in biological studies. This may indicate that it is a chemical or biological process that is responsible for the radiosensitisation effect. This study highlights the necessity to calculate the dose enhancement in more realistic scenarios, which are usually not adopted because of the extensive computing resources required.

In 2014 and 2015, Lin et al. [105, 106] published two articles on the subject of GNP radiosensitisation which encompassed kV and MV photons and therapeutic proton beams. In both papers, the dose deposited in water by secondary electrons through interactions between GNPs and ionising radiation (specifically photons and protons) was investigated.

The goal of the first paper [105] was to systematically compare the different mechanisms of GNP radiosensitisation of kV, MV photons and protons using Geant4. The focus was on the distribution of secondary electron dose distribution surrounding the NPs. The effect of energy spectrum, depth of irradiation and radiation type on radiosensitisation was investigated. A single GNP was irradiated with a particle source. The phase space file for the secondary electrons produced by ionisation and excitation within the GNP was scored on the outer surface of the GNP using Geant4 "Penelope" low energy electromagnetic physics models. The track structure outside the NP was then simulated using Geant4-DNA. The most interesting conclusion was that, for the same amount of energy absorbed in the GNP, the dose deposited by secondary electrons within several nanometres of the gold surface differs by less than 20% for kV, MV photons and protons. However, kV photons were shown to produce secondary electrons with the longest range. The authors indicated that when GNPs are internalised through endocytosis, most GNPs are accumulated in lysosomes and are not in close proximity to the nucleus. In these cases, only kV photons (which have long range secondary electrons) are capable of causing increased damage to the nucleus. If NPs could be internalised close to the nucleus or internalised within the nucleus, protons may have a similar radiosensitisation effect.

In the second article by Lin et al. [106], the Monte Carlo models were extended to investigate the biological effects of GNPs using the Local Effect Model. In this article, the same radiation sources were used from the previous work but cell specific geometries were designed. Breast cancer cells, prostate cancer cells and human brain tissue cells were modelled to quantify the radiosensitisation effect. In addition, various GNP geometries were used: GNPs randomly placed in the nucleus, GNPs randomly distributed in the whole cell, GNPs randomly distributed in the cytoplasm, GNPs distributed in the extra cellular material and GNPs distributed in both the cell and extra cellular material. The authors concluded that, proton induced cellular damage is only enhanced by GNPs when they are internalised in the nucleus. It was also discovered that for the same total mass of gold within the cell, 2 nm diameter GNPs have the largest dose enhancement effect. This is due to the higher fraction of low energy electrons escaping from the GNP and contributing to the local dose enhancement. As a final note, it was concluded that if GNPs cannot be internalised within the nucleus, no dose enhancement effect will be seen for proton treatments due to the short range of secondary electrons. When gold is internalised within the cytoplasm, the dose enhancement effect is of the same order for 6 MV X-rays and protons. kV photons showed the highest dose enhancement effect and with the greatest range.

4.4 Targeted cellular therapy

Geant4 can be adopted for simulation studies in targeted cellular therapy, thanks to its capability to handle radioactive decay and a flexible modelling of radioactive sources both in terms of geometry and generation of radiation field. The *General Particle Source* is recognised to be a flexible, easy to use feature to model particle emission of radioactive sources. Thanks to the atomic de-excitation package of Geant4, it is also possible to generate and track fluorescence X-rays and Auger electrons.

The Dose Point Kernels (DPK), which represent the radial energy deposition distribution from point isotropic sources of electrons, are of great interest in targeted cellular therapy with electron-emitting radiopharmaceuticals, because they are the basis to calculate the dose at

cellular level, required to estimate the radiobiological effect of the treatment [107]. Another quantity of interest for targeted cellular therapy is the S-value, which represents the dose to the target per unit of cumulated activity in the source region [108].

DPKs and S-values have been calculated by means of Geant4-DNA and compared to other Monte Carlo codes. This approach is valid to verify the suitability of the physics models and is justified when experimental measurements to adopt as a reference are missing.

Dose Point Kernels

Simulations of DPKs with Geant4-DNA were first simulated in liquid water by [107] using mono-energetic point source incident electrons in the 10 keV – 100 keV range. Geant4-DNA was compared to other well-known Monte Carlo codes such as CPA100, EGSnrc, FLUKA, MCNPX and PENELOPE. The reader is invited to consult [107] for code version numbers, code-specific settings used in the simulations and full original references. Using a Kolmogorov-Smirnov statistical test, the authors showed that Geant4-DNA is in agreement with EGSnrc, PENELOPE, and FLUKA and thus provides reliable results in the whole range of incident energies (10 keV - 100 keV), and that significant differences are observed with CPA100 (for 30 keV and 50 keV incident energies) and with MCNPX (at all incident energies).

In order to further improve the accuracy of Geant4-DNA physics models for electrons in the very low energy domain, a new set of physics models has been recently added to Geant4-DNA in June 2015, based on the work by Kyriakou et al. and described in [34] and in [31]. DPKs were calculated with the new set of models at low incident electron energies (100 eV and 1 keV) considering either the Geant4-DNA default models or the newly proposed models. At 100 eV, it was observed that the default Geant4-DNA models lead to a long-tail DPK caused by the too low electronic excitation cross section available by default in Geant4-DNA, as underlined in [32, 48]. At 1 keV, a good agreement is observed between both sets of models.

S-values

First attempts to calculate S-values in liquid water with Geant4-DNA are described in [109]. In this work, the authors calculated S-values for incident mono-energetic electrons (100 eV to 20 keV) and for five iodine isotopes (^{131}I to ^{135}I – the spectra were obtained from previous MC simulations) in simple spherical geometrical targets: spheres of varying radius (10 nm to 1 micrometre) for mono-energetic electrons uniformly distributed in the spheres, or colloid and follicular cells of the thyroid for the five iodine isotopes (two concentric spheres of liquid water separated by 10 micrometres: the inner sphere contains the radionuclide uniformly distributed and its radius varies between 15 and 250 micrometres, representing colloids, whereas the surrounding 10-micrometre thick spherical region represents follicular cells). Results were compared to other Monte Carlo codes (CPA100, MC4V and PENELOPE for the mono-energetic case; CELLDOSE, EGSnrc, MCNP and PENELOPE for the iodine isotopes). The reader is invited to refer to [109] for full references on these codes. The Kolmogorov-Smirnov test was also used in this study to compare Geant4-DNA to the other Monte Carlo codes. For the mono-energetic case, global statistical agreement was found with the other codes, but differences were observed for the small spheres (10 nm radius). For the colloid and follicular cells, global statistical agreement was also observed. It should be however kept in mind that some large variations of relative differences between Geant4-DNA

and these codes can be observed in some extreme cases (e.g. up to 20% in the mono-energetic case and up to 75% in the thyroid case, see further details in [109]).

An attempt to simulate the irradiation of a simplified cell was made by Geng et al.[110]; they simulated S-values in a liquid water spherical cell (radius of 10 μm) composed of a nucleus (radius of 5 μm), a cytoplasm and a membrane. Incident particles were mono-energetic electrons (1 keV to 1 MeV) and 1 MeV alpha particles. S-values are calculated for different source-target combinations. Results obtained for the electron case (cell surface as source and whole cell as target, or cell surface as source and nucleus as target) are reported to be close to MIRD data. Unfortunately, alpha particle results were not compared to other data.

More recently, Fourie et al. [111] focused on ^{123}I in order to investigate the influence of the sub-cellular localization of the Auger emitter in spheres of liquid water. They used a more realistic geometrical model of a cell: a sphere for a whole cell (radius of 5 micrometer), a spherical nucleus (radius of 4 micrometre), a 40 nm thick nuclear membrane and a 7 nm thick cellular membrane. Liquid water was used everywhere except for the membranes where they used soft tissue material (not handled by Geant4-DNA but handled by Geant4). Decay of ^{123}I was simulated using the radioactive decay module of Geant4. S-values obtained with Geant4-DNA were compared with MIRD values and with other Monte Carlo codes (ETRACK and MC4 – refer to [111] for full references) for different source – target combinations: nucleus-nucleus, cytoplasm-nucleus and whole cell – whole cell. The authors found that the maximum dose to the nucleus is delivered when the radioactivity is distributed within the cell nucleus as opposed to the cytoplasm or the whole cell. They also observed that the Geant4-DNA S-values are generally lower than the values calculated by the other MC codes (up to about 24%). The authors explained that the observed differences are mainly due to the different particle emission spectra employed by the different codes, emphasizing the influence of the radionuclide spectra on dosimetry calculations.

Finally, Sefl et al. [112] performed a very detailed study of the influence of cellular geometry on S-values. They selected mono-energetic electrons (1 keV to 100 keV) and three Auger-emitter radionuclides (^{99m}Tc, ^{111}In and ^{125}I), which spectra were obtained from taken from the AAPM Report no. 2 including the correct spectrum for ^{125}I [113]. Three geometrical models were employed in order to simulate the cell geometry: one spherical model, two ellipsoid models and an irregular shape model. All geometries are fully described in [112]; they have the same cellular and nuclear volumes as the ellipsoid cell models proposed by MIRD and these volumes are equal to the volumes of a spherical cell with radius 5 micrometres and a spherical nucleus of radius 4 micrometres. Random and uniform sampling was presented in detail and was applied to all geometrical configurations, which is especially challenging in the case of non-spherical geometries. Regarding the spherical cell geometry and the mono-energetic electrons, the authors have shown that differences between Geant4-DNA and MIRD data are the largest when the electron range becomes comparable to the size of the sphere (e.g. up to 46% for the cell surface – nucleus source – target combination). In the case of radionuclides, differences with MIRD are in the 5 – 10% range, except for the (cell surface - nucleus) combination, up to 43% for ^{125}I. These differences are attributed to the neglect of delta rays and straggling in the MIRD approach. Regarding ellipsoid geometries and mono-energetic electrons, a very good agreement has been found between Geant4-DNA and MIRD values for S-value ratios of sphere-to-ellipsoid geometries with differences less than 3%. However, differences of about 100% are obtained for the cell surface – nucleus combination at 5 keV; the origin of this discrepancy remains unknown. Regarding radioemitters, it is

found that S-values are generally lower than in the spherical case (up to 32% for ^{111}In and for the cytoplasm – nucleus combination). Lastly, for the irregular cell shape, the largest difference compared to the spherical case has been obtained for the cell surface – nucleus combination while other combinations remain small (below 5%) or moderate (up to 30%).

These works illustrate the possibilities that Geant4-DNA offers to users for dosimetry in targeted cellular therapy. Thanks to the recent addition of alternative models describing more accurately the inelastic interactions of electrons in liquid water [34] and benefitting from advanced imaging techniques such as immunofluorescence staining of individual cells or groups of cells with sub-micrometre resolution [114-116], Geant4-DNA can provide users with a set of simulation features for internal dosimetry in very realistic geometrical models of cells for a variety of incident radiation qualities.

4.5 Geant4-DNA coupled with tracking in magnetic fields

With the advent of magnetic resonance imaging MRI-guided radiation therapy, it is becoming increasingly important to consider the potential influence of a magnetic field on ionising radiation at nanoscale as this can impact the radiobiological effectiveness of the therapeutic radiation beam. Bug et al, [117] and Lazarakis et al. [72] studied the effect of the magnetic field on the track structure of electrons, protons and alpha particles on the cluster size distribution in a DNA segment, modelled as a liquid water cylinder with nanometric sizes. The intensity of the magnetic field was varied from 0 to 14 T. The Geant4-DNA Package was adopted to model the physics interactions of particles in the set-up. The studies showed no significant impact of the magnetic field on the track structure, cluster size distribution and probability of producing a DSB. However, it is important to note that in Geant4 the presence of the magnetic field can impact the trajectory of charged particles only, and not the cross sections of the physical processes. It has been shown that molecules may align with magnetic field [118], while the Geant4-DNA cross sections assume that the hit direction is random. If the hit direction is not random then it could lead to significant differences in cross sections, particularly differential cross sections (kinetic energy of delta electrons etc.).

5. Future

5.1 Directions and Conclusions

One of the main achievements of Geant4-DNA is to extend the general purpose Geant4 Monte Carlo toolkit for the simulation of ionising radiation physical interactions with biological systems at the cellular and DNA level (i.e. micro and nano dosimetry).

As demonstrated in this review, the scope of potential applications includes X-ray radiotherapy, hadron therapy, NP radiosensitisation, targeted cellular therapy and other radiobiology applications. In addition, the extensive Geant4 functionality allowing the modelling of various geometries and the convenient user interface enabling the combination of physics models definitively encourages the use of Geant4-DNA in the medical physics community. Its free availability and open source access undoubtedly supported its widespread adoption.

There is still, however, scope and need for further development. For example, in order to use Geant4-DNA for early damage simulation in radiotherapy, it is pivotal to fully simulate radiation chemistry and the related production of indirect damage. As briefly explained, Geant4-DNA offers a full set of prototype features allowing the simulation of water

radiolysis from ionising radiation, up to one microsecond after irradiation. Pachnerova et al. [119] performed the first validation of Geant4-DNA water radiolysis simulation capabilities for incident 15-30 MeV protons. They found an acceptable agreement between simulated radiochemical yields for hydroxyl radicals as a function of time versus experimental measurements. Such validation studies are strongly needed to further evaluate Geant4-DNA modelling accuracy for water radiolysis. Another recent application of Geant4-DNA, including water radiolysis simulation, was recently presented by Tran et al. [120] for the Geant4 simulation of molecular species production around a single 50 nm sphere of gold irradiated by incident MeV protons. The authors estimated the Dose Enhancement Factor and Radiolysis Enhancement Factor of the gold nanosphere compared to a liquid water nanosphere, as a function of radial distance from the sphere; they showed preliminary results demonstrating similar trends for the simulated incident proton energy range and underlined current Geant4 limitations. More realistic mechanistic simulations will be required to fully investigate the possible potential of NPs in radiotherapy, in particular, the development of Geant4-DNA discrete models for the description of electrons interactions in gold NPs.

These recent developments have clearly paved the way for a variety of new Geant4-DNA applications at the nanometer scale requiring the simulation of physical, physicochemical and chemical interactions.

Geant4-DNA operates in a very low energy region that is governed by significant theoretical and experimental complexity. Any theoretical calculations must take into account detailed dielectric structure of the interacting material. Sometimes, for simplification purpose, approximations, assumptions, semi-empirical models must be used. In parallel, experimental measurements below 100 eV are needed to fully validate the models against experimental data. However, such measurements are difficult and are subject to practical constraints. There is a lack of experimental data in liquid water in this energy range and new measurements are still needed. However, while all models have their own limitations, the Geant4-DNA models provide reasonable agreement when compared to literature data and will continue to be improved as new data (e.g. very low energy cross-sections) become available.

In summary, Monte Carlo methods have been explored and used for years as a tool for precise dosimetry as an alternative to analytical methods or for verification of experimental measurements. Geant4-DNA is a very promising and exciting track structure simulation tool for use in radiobiology and micro/nanodosimetry. It is also an excellent example of multidisciplinary and international collaboration involving physicists, theoreticians, radiobiologists, chemists and others from a large number of institutions worldwide. We can be nothing but excited to see further development of this toolkit.

Acknowledgements:

The authors are grateful to Dr Y. Perrot for fruitful discussions about the Geant4-DNA clustering example. The authors also thank Dr F. Semsarha for providing Figure 2.

References:

[1] Chadwick K, Leenhouts H. A molecular theory of cell survival. Phys Med Biol. 1973;18:78.
[2] Berger MJ. Monte Carlo calculation of the penetration and diffusion of fast charged particles. Methods in computational physics. 1963;1:135-215.

[3] Nelson WR, Hirayama H, Rogers DW. EGS4 code system. Stanford Linear Accelerator Center, Menlo Park, CA (USA); 1985.
[4] Baro J, Sempau J, Fernández-Varea J, Salvat F. PENELOPE: an algorithm for Monte Carlo simulation of the penetration and energy loss of electrons and positrons in matter. Nucl Instr Meth Phys Res B: Beam Interactions with Materials and Atoms. 1995;100:31-46.
[5] Agostinelli S, Allison J, Amako Ka, Apostolakis J, Araujo H, Arce P, et al. Geant4—a simulation toolkit. Nucl Instr Meth Phys Res A. 2003;506:250-303.
[6] Allison J, Amako K, Apostolakis J, Araujo H, Arce Dubois P, Asai M, et al. Geant4 developments and applications. IEEE Trans Nuc Sc. 2006;53:270-8.
[7] Allison J, Amako K, Apostolakis J, Arce P, Asai M, Aso T, et al. Recent developments in Geant4. Nucl Instr Meth Phys Res A. 2016:40 pages.
[8] MCNP. MCNP 5-1.40 RSICC Release Notes, LA-UR-05-8617. 2005.
[9] Grosswendt B. Formation of ionization clusters in nanometric structures of propane-based tissue-equivalent gas or liquid water by electrons and α-particles. Radiat Environ Biophys. 2002;41:103-12.
[10] Friedland W, Dingfelder M, Kundrát P, Jacob P. Track structures, DNA targets and radiation effects in the biophysical Monte Carlo simulation code PARTRAC. Mutat Res. 2011;711:28-40.
[11] Uehara S, Nikjoo H, Goodhead D. Cross-sections for water vapour for the Monte Carlo electron track structure code from 10 eV to the MeV region. Phys Med Biol. 1993;38:1841.
[12] Wälzlein C, Scifoni E, Krämer M, Durante M. Simulations of dose enhancement for heavy atom nanoparticles irradiated by protons. Phys Med Biol. 2014;59:1441.
[13] Plante I, Cucinotta FA. Monte-Carlo simulation of ionizing radiation tracks. Application of Monte Carlo methods in biology, medicine and other fields of science InTech, Rijeka, Croatia. 2011:315-56.
[14] Nikjoo H, Emfietzoglou D, Watanabe R, Uehara S. Can Monte Carlo track structure codes reveal reaction mechanism in DNA damage and improve radiation therapy? Rad Phys Chem. 2008;77:1270-9.
[15] Nikjoo H, Goodhead D. Track structure analysis illustrating the prominent role of low-energy electrons in radiobiological effects of low-LET radiations. Phys Med Biol. 1991;36:229.
[16] Bardiès M, Pihet P. Dosimetry and microdosimetry of targeted radiotherapy. Curr Pharm Des. 2000;6:1469-502.
[17] Huang C-Y, Oborn BM, Guatelli S, Allen BJ. Monte Carlo calculation of the maximum therapeutic gain of tumor antivascular alpha therapy. Med Phys. 2012;39:1282-8.
[18] McMahon SJ, Hyland WB, Muir MF, Coulter JA, Jain S, Butterworth KT, et al. Biological consequences of nanoscale energy deposition near irradiated heavy atom nanoparticles. Scientific reports. 2011;1.
[19] Elsässer T, Krämer M, Scholz M. Accuracy of the local effect model for the prediction of biologic effects of carbon ion beams in vitro and in vivo. Int. J. Radiation Oncology Biol. Phys. 2008;71:866-72.
[20] Kanai T, Endo M, Minohara S, Miyahara N, Koyama-ito H, Tomura H, et al. Biophysical characteristics of HIMAC clinical irradiation system for heavy-ion radiation therapy. Int J Radiat Oncol Biol Phys. 1999;44:201-10.
[21] Hawkins R. A statistical theory of cell killing by radiation of varying linear energy transfer. Rad Res. 1994;140:366-74.
[22] Hawkins R. A microdosimetric-kinetic model for the effect of non-poisson distribution of lethal lesions on the variation of RBE with LET. Rad Res. 2003;160:61-9.
[23] Nikjoo H, Uehara S, Wilson W, Hoshi M, Goodhead D. Track structure in radiation biology: theory and applications. Int J Radiat Biol. 1998;73:355-64.

[24] El Naqa I, Pater P, Seuntjens J. Monte Carlo role in radiobiological modelling of radiotherapy outcomes. Phys Med Biol 2012;57:R75-97.
[25] Palmans H, Rabus H, Belchior A, Bug M, Galer S, Giesen U, et al. Future development of biologically relevant dosimetry. Brit J Radiol. 2015;88:20140392.
[26] Gervais B, Beuve M, Olivera G, Galassi M, Rivarola R. Production of HO2 and O2 by multipleionization in water radiolysis by swift carbon ions. Chem Phys Lett. 2005;410:330–4.
[27] Gervais B, Beuve M, Olivera G, Galassi M. Numerical simulation of multiple ionization and high LET effects in liquid water radiolysis. Radiat Phys Chem. 2006;75:493-513.
[28] Li J, Li C, Qiu R, Yan C, Xie W, Wu Z, et al. DNA strand breaks induced by electrons simulated with nanodosimetry Monte Carlo simulation code. Radiat Prot Dosimetry. 2015;166:38-43.
[29] Plante I, Cucinotta F. Cross sections for the interactions of 1 eV–100 MeV electrons in liquid water and application to Monte-Carlo simulation of HZE radiation tracks. New J Phys. 2009;11:24 pp.
[30] Plante I, Cucinotta F. Ionization and excitation cross sections for the interaction of HZE particles in liquid water and application to Monte Carlo simulation of radiation tracks. New J Phys 2008;10:15 pp.
[31] Bernal MA, Bordage MC, Brown JM, Davidkova M, Delage E, El Bitar Z, et al. Track structure modeling in liquid water: A review of the Geant4-DNA very low energy extension of the Geant4 Monte Carlo simulation toolkit. Physica Medica. 2015;31:861-74.
[32] Incerti S, Ivanchenko A, Karamitros M, Mantero A, Moretto P, Tran H, et al. Comparison of GEANT4 very low energy cross section models with experimental data in water. Med Phys. 2010;37:4692-708.
[33] Chauvie S, Francis Z, Guatelli S, Incerti S, Mascialino B, Moretto P, et al. Geant4 physics processes for microdosimetry simulation: design foundation and implementation of the first set of models. IEEE Transactions on Nuc Sc. 2007;54:2619-28.
[34] Kyriakou I, Incerti S, Francis Z. Technical Note: Improvements in GEANT4 energy-loss model and the effect on low-energy electron transport in liquid water. Med Phys. 2015;42:3870-6.
[35] Kyriakou I, Sefl M, Nourry V, Incerti S. The impact of new Geant4-DNA cross section models on electron track structure simulations in liquid water,. J Appl Phys 2016;194902.
[36] Francis Z, Incerti S, Capra R, Mascialino B, Montarou G, Stepan V, et al. Molecular scale track structure simulations in liquid water using the Geant4-DNA Monte-Carlo processes. Appl Radiat Isot. 2011a;69:220-6.
[37] Dingfelder M, Inokuti M, Paretzke H. Inelastic-collision cross sections of liquid water for interactions of energetic protons. Radiat Phys Chem. 2000;59:255-75.
[38] Tran H, El Bitar Z, Champion C, Karamitros M, Bernal M, Francis Z, et al. Modeling proton and alpha elastic scattering in liquid water in Geant4-DNA. Nucl Instrum and Meth B. 22015;343:132-7.
[39] Dingfelder M, Paretzke H, Toburen L. "An effective charge scaling model for ionization of partially dressed helium ions with liquid water. Proceedings of the Monte Carlo 2005 Topical Meeting, Chattanooga, TN. 2005.
[40] Francis Z, Incerti S, Ivanchenko V, Champion C, Karamitros M, Bernal MA, et al. Monte Carlo simulation of energy-deposit clustering for ions of the same LET in liquid water. Phys Med Biol. 2012;57:209.
[41] Karamitros M, Luan S, Bernal M, Allison J, Baldacchino G, Davidkova M, et al. Diffusion-controlled reactions modeling in Geant4-DNA. J Comput Phys. 2014;274:841-82.
[42] Karamitros M, Mantero A, Incerti S, Friedland W, Baldacchino G, Barberet P, et al. Modeling radiation chemistry in the Geant4 toolkit. Prog Nucl Sci Tech. 2011;2:503-8.
[43] Hirayama R, Ito A, Tomita M, Tsukada T, Yatagai F, Noguchi M, et al. Contributions of direct and indirect actions in cell killing by high-LET radiations. Rad Res. 2009;171:212-8.

[44] Bernal M, deAlmeida C, Incerti S, Champion C, Ivanchenko V, Francis Z. The influence of DNA configuration on the direct strand break yield. Comput Math Methods Med. 2015a.
[45] Francis Z, Stypczynska A. Clustering algorithms in radiobiology and DNA damage quantification. Data Mining: New Technologies, Benefits and Privacy Concerns. 2013.
[46] Francis Z, Villagrasa C, Clairand I. Simulation of DNA damage clustering after proton irradiation using an adapted DBSCAN algorithm. Comput Meth Prog Bio. 2011c;101:265-70.
[47] Ester M, Kriegel H, Sander J, Xu X. A density-based algorithm for discovering clusters in large spatial databases with noise. Proc 2nd Intl Conf Knowledge Discovery and Data Mining. 1996:226-31.
[48] Douglass M, Penfold S, Bezak E. Preliminary Investigation of Microdosimetric Track Structure Physics Models in Geant4-DNA and RITRACKS. Comput Math Methods Med. 2015a;2015.
[49] Batmunkh M, Bayarchimeg L, Lkhagva O, Belov O. Cluster analysis of HZE particle tracks as applied to space radiobiology problems. Phys Part Nuclei Lett. 2013;10:854-9.
[50] Bernal M, Sampaio C, Incerti S, Champion C, Nieminen P. The invariance of the total direct DNA strand break yield. Med Phys. 2011;38:4147-53.
[51] Sempau J, Acosta E, Baro J, Fernandez-Varea J, Salvat F. An algorithm for Monte Carlo simulation of the coupled electron-photon transport. Nucl Instr Meth Phys Res B. 1997:377-90.
[52] Bernal M, Liendo J. An investigation on the capabilities of the PENELOPE MC code in nanodosimetry. Med Phys. 2009;36:620-5.
[53] Incerti S, Champion C, Tran H, Karamitros M, Bernal M, Francis Z, et al. Energy deposition in small-scale targets of liquid water using the very low energy electromagnetic physics processes of the Geant4 toolkit. Nucl Instr Meth Phys Res B. 2013;306:158-64.
[54] Raisali G, Mirzakhanian L, Masoudi SF, Semsarha F. Calculation of DNA strand breaks due to direct and indirect effects of Auger electrons from incorporated 123I and 125I radionuclides using the Geant4 computer code. Int J Radiat Biol. 2013;89:57-64.
[55] Semsarha F, Goliaei B, Raisali G, Khalafi H, Mirzakhanian L. An investigation on the radiation sensitivity of DNA conformations to 60 Co gamma rays by using Geant4 toolkit. Nucl. Instr. Meth. Phys. Res B. 2014;323:75-81.
[56] Tajik M, Rozatian AS, Semsarha F. Calculation of direct effects of 60 Co gamma rays on the different DNA structural levels: A simulation study using the Geant4-DNA toolkit. Nucl Instr Meth Phys Res B. 2015;346:53-60.
[57] Tajik M, Rozatian AS, Semsarha F. Simulation of ultrasoft X-rays induced DNA damage using the Geant4 Monte Carlo toolkit. Nucl Instr Meth Phys Res B. 2015a;342:258-65.
[58] Pomplun E. A new DNA target model for track structure calculations and its first application to I-125 Auger electrons. Int J Radiat Biol. 1991;59:625-42.
[59] Charlton D, Humm J. A method of calculating initial DNA strand breakage following the decay of incorporated 125I. Int J Radiat Biol. 1988;53:353-65.
[60] Li J-L, Li C-Y, Qiu R, Yan C-C, Xie W-Z, Zeng Z, et al. Comparison of direct DNA strand breaks induced by low energy electrons with different inelastic cross sections. Nucl Instr Meth Phys Res B. 2013;311:27-36.
[61] Bernal M, Sikansi D, Cavalcante F, Incerti S, Champion C, Ivanchenko V, et al. An atomistic geometrical model of the B-DNA configuration for DNA–radiation interaction simulations. Comp Phys Comm. 2013;184:2840-7.
[62] Bernal M, Sikansi D, Cavalcante F, Incerti S, Champion C, Ivanchenko V, et al. Performance of a new atomistic geometrical model of the B-DNA configuration for DNA-radiation interaction simulations. Journal of Physics: Conference Series: IOP Publishing; 2014. p. 012150.

[63] Friedland W, Jacob P, Bernhardt P, Paretzke H, Dingfelder M. Simulation of DNA damage after proton irradiation. Rad Res. 2003;159:401-10.
[64] Xie W, Li J, Li C, Qiu R, Yan C, Zeng Z. Comparison of direct DNA strand break simulated with different DNA models. Rad Prot Dosimetry. 2013;156:283-8.
[65] Delage E, Pham QT, Karamitros M, Payno H, Stepan V, Incerti S, et al. PDB4DNA: Implementation of DNA geometry from the Protein Data Bank (PDB) description for Geant4-DNA Monte-Carlo simulations. Comp Phys Comm. 2015;192:282-8.
[66] Meylan S, Vimont U, Incerti S, Clairand I, Villagrasa C. Geant4-DNA simulations using complex DNA geometries generated by the DnaFabric tool. Comp Phys Comm. 2016;204:159-69.
[67] Bueno M, Schulte R, Meylan S, Villagrasa C. PO-0824: Influence of the biological target volume modeling on ionization cluster-size distributions using Geant4-DNA. Radiother Oncol. 2015;115:S415-S6.
[68] Bueno M, Schulte R, Meylan S, Villagrasa C. Influence of the geometrical detail in the description of DNA and the scoring method of ionization clustering on nanodosimetric parameters of track structure: a Monte Carlo study using Geant4-DNA. Phys Med Biol. 2015a;60:8583.
[69] Dos Santos M, Clairand I, Gruel G, Barquinero J, Incerti S, Villagrasa C. Influence of chromatin condensation on the number of direct DSB damages induced by ions studied using a Monte Carlo code. Radiat Prot Dosimetry. 2014a:ncu029.
[70] Dos Santos M, Villagrasa C, Clairand I. Influence of the chromatin density on the number of direct clustered damages calculated for proton and alpha irradiations using a Monte Carlo code. Prog Nucl Sci Tech. 2014;4:449-53.
[71] Dos Santos M, Villagrasa C, Clairand I, Incerti S. Influence of the DNA density on the number of clustered damages created by protons of different energies. Nucl Instr Meth Phys Res B. 2013;298:47-54.
[72] Lazarakis P, Bug M, Gargioni E, Guatelli S, Rabus H, Rosenfeld AB. Comparison of nanodosimetric parameters of track structure calculated by the Monte Carlo codes Geant4-DNA and PTra. Phys Med Biol. 2012;57:1231.
[73] Barberet P, Seznec H. Advances in microbeam technologies and applications to radiation biology. Radiat Prot Dosimetry. 2015:ncv192.
[74] Bourret S, Vianna F, Devès G, Atallah V, Moretto P, Seznec H, et al. Fluorescence time-lapse imaging of single cells targeted with a focused scanning charged-particle microbeam. Nucl Instr Meth Phys B. 2014;325:27-34.
[75] Humm J, Chin L. A model of cell inactivation by alpha-particle internal emitters. Rad Res. 1993;134:143-50.
[76] Douglass M, Bezak E, Penfold S. Development of a randomized 3D cell model for Monte Carlo microdosimetry simulations. Med Phys. 2012;39:3509-19.
[77] Incerti S, Gault N, Habchi C, Lefaix J, Moretto P, Poncy J, et al. A comparison of cellular irradiation techniques with alpha particles using the Geant4 Monte Carlo simulation toolkit. Radiat Prot Dosimetry. 2006;122:327-9.
[78] Kvinnsland Y, Stokke T, Aurlien E. Radioimmunotherapy with alpha-particle emitters: microdosimetry of cells with a heterogeneous antigen expression and with various diameters of cells and nuclei. Rad Res. 2001;155:288-96.
[79] Kuncic Z. Advances in computational radiation biophysics for cancer therapy: simulating nano-scale damage by low-energy electrons. Biophysical Reviews and Letters. 2015;10:25-36.
[80] McNamara A, Oelfke U, Kuncic Z. Revealing the underlying mechanism of microbeam radiation therapy with low energy Monte Carlo simulations. Journal of Physics: Conference Series: IOP Publishing; 2014. p. 012018.

[81] McNamara AL, Guatelli S, Prokopovich DA, Reinhard MI, Rosenfeld AB. A comparison of x-ray and proton beam low energy secondary electron track structures using the low energy models of Geant4. Int J Radiat Biol. 2012;88:164-70.
[82] Paganetti H. Relative biological effectiveness (RBE) values for proton beam therapy. Variations as a function of biological endpoint, dose, and linear energy transfer. Phys Med Biol. 2014;59:R419.
[83] Sørensen BS, Overgaard J, Bassler N. In vitro RBE-LET dependence for multiple particle types. Acta Oncologica. 2011;50:757-62.
[84] Paganetti H, Niemierko A, Ancukiewicz M, Gerweck LE, Goitein M, Loeffler JS, et al. Relative biological effectiveness (RBE) values for proton beam therapy. International Journal of Radiation Oncology*Biology*Physics. 2002;53:407-21.
[85] Jäkel O, Krämer M, Schulz-Ertner D, Heeg P, Karger CP, Didinger B, et al. Treatment planning for carbon ion radiotherapy in Germany: Review of clinical trials and treatment planning studies. Radiotherapy and Oncology. 2004;73, Supplement 2:S86-S91.
[86] Bug MU, Rabus H, Rosenfeld AB. Electron emission from amorphous solid water after proton impact: Benchmarking PTra and Geant4 track structure Monte Carlo simulations. Radiat Phys Chem. 2012;81:1804-12.
[87] Toburen LH, McLawhorn SL, McLawhorn RA, Carnes KD, Dingfelder M, Shinpaugh JL. Electron Emission from Amorphous Solid Water Induced by Passage of Energetic Protons and Fluorine Ions. Rad Res. 2010;174:107-18.
[88] Wang H, Vassiliev ON. Radial dose distributions from protons of therapeutic energies calculated with Geant4-DNA. Phys Med Biol. 2014;59:3657.
[89] Paganetti H, Goitein M. Biophysical modelling of proton radiation effects based on amorphous track models. Int J Radiat Biol. 2001;77:911-28.
[90] Francis Z, Incerti S, Karamitros M, Tran HN, Villagrasa C. Stopping power and ranges of electrons, protons and alpha particles in liquid water using the Geant4-DNA package. Nucl Instr Meth Phys Res B. 2011;269:2307-11.
[91] ICRU. Stopping Power and Ranges for Protons and Alpha Particles. Bethesda, Maryland, USA1993.
[92] Borak TB, Doke T, Fuse T, Guetersloh S, Heilbronn L, Hara K, et al. Comparisons of LET Distributions for Protons with Energies between 50 and 200 MeV Determined Using a Spherical Tissue-Equivalent Proportional Counter (TEPC) and a Position-Sensitive Silicon Spectrometer (RRMD-III). Rad Res. 2004;162:687-92.
[93] Champion C, Galassi ME, Weck PF, Incerti S, Rivarola RD, Fojón O, et al. Proton-induced ionization of isolated uracil molecules: A theory/experiment confrontation. Nucl Instr Meth Phys Res B. 2013a;314:66-70.
[94] Champion C, Incerti S, Tran HN, Karamitros M, Shin JI, Lee SB, et al. Proton transport in water and DNA components: A Geant4 Monte Carlo simulation. Nucl Instr Meth Phys Res B. 2013;306:165-8.
[95] Pham Q, Anne A, Bony M, Delage E, Donnarieix D, Dufaure A, et al. Coupling of Geant4-DNA physics models into the GATE Monte Carlo platform: Evaluation of radiation-induced damage for clinical and preclinical radiation therapy beams. Nucl Instr Meth Phys Res B. 2015;353:46-55.
[96] Jan S, Santin G, Strul D, Staelens S, Assié K, Autret D, et al. GATE: a simulation toolkit for PET and SPECT. Phys Med Biol. 2004;49:4543.
[97] Francis Z, Seif E, Incerti S, Champion C, Karamitros M, Bernal MA, et al. Carbon ion fragmentation effects on the nanometric level behind the Bragg peak depth. Phys Med Biol. 2014;59:7691.
[98] Scholz M, Kellerer MA, Kraft-Weyrather W, Kraft G. Computation of cell survival in heavy ion beams for therapy. Radiat Environ Bioph. 1997;36:59-66.

[99] Casiraghi M, Schulte RW. Nanodosimetry-Based Plan Optimization for Particle Therapy. Comput Math Methods Med. 2015;2015:13.
[100] Guatelli S. Predicting the physical and physico/chemical mechanism of DNA damage: The Geant4-DNA Project. 14th International Workshop on Radiation Damage to DNA. Melbourne, Australia2016.
[101] McMahon SJ, Paganetti H, Prise KM. Optimising element choice for nanoparticle radiosensitisers. Nanoscale. 2016;8:581-9.
[102] Douglass M, Bezak E, Penfold S. Development of a radiation track structure clustering algorithm for the prediction of DNA DSB yields and radiation induced cell death in Eukaryotic cells. Phys Med Biol. 2015;60:3217.
[103] Douglass M, Bezak E, Penfold S. Monte Carlo investigation of the increased radiation deposition due to gold nanoparticles using kilovoltage and megavoltage photons in a 3D randomized cell model. Med Phys. 2013;40:071710.
[104] Martínez-Rovira I, Prezado Y. Evaluation of the local dose enhancement in the combination of proton therapy and nanoparticles. Med Phys. 2015;42:6703-10.
[105] Lin Y, McMahon SJ, Scarpelli M, Paganetti H, Schuemann J. Comparing gold nano-particle enhanced radiotherapy with protons, megavoltage photons and kilovoltage photons: a Monte Carlo simulation. Phys Med Biol. 2014;59:7675.
[106] Lin Y, McMahon SJ, Paganetti H, Schuemann J. Biological modeling of gold nanoparticle enhanced radiotherapy for proton therapy. Phys Med Biol. 2015;60:4149.
[107] Champion C, Incerti S, Perrot Y, Delorme R, Bordage M-C, Bardiès M, et al. Dose point kernels in liquid water: an intra-comparison between GEANT4-DNA and a variety of Monte Carlo codes. Appl Radiat Isot. 2014;83:137-41.
[108] Goddu SM, Howell R, Bouchet L, Bolch W, Rao D. MIRD cellular S values. Reston, VA: Society of Nuclear Medicine. 1997.
[109] André T, Morini F, Karamitros M, Delorme R, Le Loirec C, Campos L, et al. Comparison of Geant4-DNA simulation of S-values with other Monte Carlo codes. Nucl Instr Meth Phys Res B. 2014;319:87-94.
[110] Geng J-P, Tian-Guang C, Duo-Fang L, Hai-Long A, Ying-Rong H, Jin L, et al. Calculation of the Physical and Microdosimetric Parameters of Electron and Alpha-Particle Radiation Using Monte Carlo Simulations. Chinese Phys Lett. 2014;31:038701.
[111] Fourie H, Newman R, Slabbert J. Microdosimetry of the Auger electron emitting 123I radionuclide using Geant4-DNA simulations. Phys Med Biol. 2015;60:3333.
[112] Šefl M, Incerti S, Papamichael G, Emfietzoglou D. Calculation of cellular S-values using Geant4-DNA: the effect of cell geometry. Appl Radiat Isot. 2015;104:113-23.
[113] Howell RW. Radiation spectra for Auger-electron emitting radionuclides: Report No. 2 of AAPM Nuclear Medicine Task Group No. 6. Med Phys. 1992;19:1371-83.
[114] Arnaud F, Paillas S, Pouget J, Incerti S, Bardiès M, Bordage M. Complex cell geometry and sources distribution model for Monte Carlo single cell dosimetry with iodine 125 radioimmunotherapy. Nucl Instr Meth Phys Res B. 2016;366:227-33.
[115] Barberet P, Vianna F, Karamitros M, Brun T, Gordillo N, Moretto P, et al. Monte-Carlo dosimetry on a realistic cell monolayer geometry exposed to alpha particles. Phys Med Biol. 2012;57:2189.
[116] Incerti S, Seznec H, Simon M, Barberet P, Habchi C, Moretto P. Monte Carlo dosimetry for targeted irradiation of individual cells using a microbeam facility. Radiat Prot Dosimetry. 2009;133:2-11.
[117] Bug M, Gargioni E, Guatelli S, Incerti S, Rabus H, Schulte R, et al. Effect of a magnetic field on the track structure of low-energy electrons: a Monte Carlo study. Eur Phys J D. 2010;60:85-92.

[118] Hill R, Sedman VL, Allen S, Williams P, Paoli M, Adler-Abramovich L, et al. Alignment of aromatic peptide tubes in strong magnetic fields. Advanced Materials. 2007;19:4474-9.
[119] Pachnerova Brabcová K, Štěpán V, Karamitros M, Karabín M, Dostálek P, Incerti S, et al. Contribution of indirect effects to clustered damage in DNA irradiated with protons. Radiat Prot Dosimetry. 2015;166:44-8.
[120] Tran H, Karamitros M, Ivanchenko V, Guatelli S, McKinnon S, Murakami K, et al. Geant4 Monte Carlo simulation of absorbed dose and radiolysis yields enhancement from a gold nanoparticle under MeV proton irradiation. Nucl Instr Meth Phys Res B. 2016;373:126-39.